INTERPRETATION OF POLARISATION BEHAVIOUR OF RADAR WAVES TRANSMITTED THROUGH ANTARCTIC ICE SHELVES.

C S M Doake[1], H F J Corr [1], A Jenkins[1] , K W Nicholls[1] and C Stewart[1]
[1]British Antarctic Survey, Natural Environment Research Council, Madingley Road, Cambridge, CB3 0ET, UK.
csmd@bas.ac.uk

ABSTRACT

We have collected polarimetric ice sounding radar data on Brunt, George VI and Ronne ice shelves using a vector network analyser as a continuous wave step-frequency radar. Being a wideband phase sensitive instrument, the radar allowed the vectorial nature of the interaction between radio waves and the ice and reflecting surface to be explored. Single crystals of ice are birefringent not only at optical frequencies but also at radar ones, so in an ice sheet the average crystal orientation fabric determines the overall level of birefringence. The polarisation of radio waves is changed by the birefringent nature of the ice and by the reflecting surface, whether an internal layer or the basal boundary. By transmitting and receiving on orthogonal linearly polarised aerials, we could use a scattering matrix approach to determine parameters related to the physical properties and nature of both the ice and the reflecting surface. The polarisation behaviour will have to be allowed for when processing ice penetrating SAR data.

1 INTRODUCTION

The depolarisation behaviour of ice sheets on radar waves transmitted through them and reflected from the base or from internal horizons has been recognised since the early days of radio-echo sounding in the 1960s [1]. Several studies have been made of the phenomenon but the relatively unsophisticated equipment in use until recently meant that only power could be measured, not phase [2-10]. Extracting relevant physical parameters required aerials to be rotated to gather sufficient measurements. Hargreaves [9, 10] rotated crossed dipoles and obtained reflections from internal layers in Greenland. He interpreted his results in terms of an overall birefringence of the ice and established the relationship between a crystal orientation fabric and the birefringence. Woodruff and Doake [6] rotated separate transmitting and receiving dipoles over Bach Ice Shelf in the Antarctic Peninsula to distinguish between grounded and floating ice.

By measuring phase as well as amplitude, it is possible to construct a polarimetric radar that requires only orthogonal aerials, making it suitable for airborne use. It is possible to simulate from measurements on orthogonal linearly polarised aerials the observations that would have been made at any other polarisation state, for example different orientations of linearly polarised aerials or even circularly polarised ones.

Polarimetric radars have been flown on aircraft (e.g. AirSAR, CARABAS, E-SAR, SASAR, etc) and satellites (e.g. ERS1/2, RADARSAT, etc) for studying the earth's surface. They tend to be associated with synthetic aperture radars (SAR) and operate at frequencies too high for significant penetration into ice sheets, although P-band (~450 MHz) or VHF (~140 MHz) SARs might be successful if flown at suitable terrain clearances. There are also ground based polarimetric systems for investigating small regions. Polarimetric information is normally used to help discriminate targets in SAR images rather than infer physical properties of the target surfaces.

Early attempts with a ground based radar to produce SAR images of glacier beds were time consuming [11-13] and covered only a very small area, so the technique was not pursued. With modern radar equipment there seems no real impediment to achieving our goal of imaging the bed of a glacier. This ability would revolutionise the interpretation of basal conditions on ice sheets, ice streams and ice shelves. However, ground based systems would have limited areal coverage and airborne systems would require lower operating frequencies than normally used for airborne SARs. In either case there is the problem of correcting for distortion caused by refraction and birefringence in the ice. Polarimetric information will be needed to sharpen SAR images.

Both the ice and reflecting surfaces are of interest, the ice sheet because of the crystal fabric responsible for the birefringence, which in turn is a product of the strain/stress history of the ice sheet, and the reflecting surfaces for the insight they can give into internal processes and the nature and conditions of the basal zone. Fabric evolution can be

included in an ice sheet model to predict the birefringence, which can be checked by field measurement. Such modelling work will also have to include realistic reflecting characteristics for basal and internal layers. Even if the polarisation parameters are not reproduced precisely, their variation and pattern of change with position over an area can be compared.

In this paper, we concentrate on describing the polarisation behaviour of radio waves propagating through and reflected within and at the base of ice sheets. Ground based radar data on ice shelves are analysed using a scattering matrix approach to determine physical properties of both the ice and the reflecting surfaces.

2 PROPAGATION OF ELECTROMAGNETIC WAVES IN ICE

Single crystals of naturally occurring ice Ih are uniaxially birefringent with the optic axis coinciding with the crystallographic c-axis. We make the assumption that a polycrystalline ice sheet also exhibits a birefringent behaviour, with a strength determined by the crystal orientation fabric [10]. Plane wave solutions of Maxwell's equations show that only two directions are allowed for propagation, the extraordinary wave in the plane containing the optic axis and the ordinary wave in the plane perpendicular to it [10]. Ice is optically positive, so that the velocity of the ordinary ray is greater than the extraordinary ray. The propagation vectors are different in the two directions, leading to a change in phase between the field components such that an incident wave that is linearly polarised will become elliptically polarised after passing through the medium.

2.1 Sinclair scattering matrix

Coherent backscatter of completely polarised plane electromagnetic waves from deterministic targets is described by a 2x2 complex scattering matrix called the Sinclair matrix [14], which is the analogue of the Jones matrix in optical or forward scattering (i.e. transmission) situations. In the 'Back Scatter Alignment' (BSA) convention [15], which uses a common 2-dimensional orthonormal polarization basis for the transmitted and received waves, the Sinclair matrix is symmetric for reciprocal targets. A brief derivation and description follows.

Let $\mathbf{E}(z)$ be a complex vector describing a plane harmonic electromagnetic wave travelling in the z direction. In a Cartesian coordinate frame (x, y) transverse to z, the total electric field vector $\mathbf{E}$ is given by

$$\mathbf{E} = E_x \mathbf{x} + E_y \mathbf{y},$$

with the field components given by

$$E_x = E_{x0} \exp i(\omega t - kz)$$
$$E_y = E_{y0} \exp i(\omega t - kz + \delta)$$

where ω is the angular frequency, t is time, k is the wavenumber, δ is the phase difference between components, E_{x0}, E_{y0} are the amplitudes of the components and $\mathbf{x}$, $\mathbf{y}$ are unit vectors in the x, y directions respectively. The column vector $\mathbf{E} = [E_x, E_y]^T = [E_{x0}, E_{y0} \exp(i\delta)]^T$, where the common factor $\exp i(\omega t - kz)$ has been removed, is called the Jones vector ($[\bullet]^T$ is transpose).

In the monostatic radar case, by introducing at the aerial a common Cartesian coordinate system for the domain and range [16, p5] of the scattering matrix, S_M, the backward scattering process can be described by the field equation for radar polarimetry [14]

$$\mathbf{E^s} = S_M \mathbf{E^i} \tag{1}$$

where the superscripts s and i denote scattering and incidence. The Sinclair scattering matrix is given by:

$$S_M = S_M^T = \begin{bmatrix} s_{11} & s_x \\ s_x & s_{22} \end{bmatrix} \qquad s_x = s_{12} = s_{21} \ .$$

The Sinclair matrix S_M links the forward travelling wave with the backscattered one, in the same 2-dimensional coordinate system orthogonal to the direction of travel.

In physical optics, an eigenmode analysis of the scattering matrix gives the two (complex) eigenvectors corresponding to the two orthogonal polarisation states which are transmitted and received at the same polarisation state, while the

eigenvalues are the corresponding (complex) amplitudes of these two states. A similar relationship exists for radar polarimetry, where however, the polarisation invariants are determined from the coneigenvector equation [16, p245], known in the radar community as Kennaugh's pseudo-eigenvalue equation [14],

$$S_M \mathbf{x} = \lambda \mathbf{x}^*$$ (2)

where $\mathbf{x}^*$ is the complex conjugate of the coneigenvector $\mathbf{x}$ and λ is a coneigenvector of S_M. Eq. 2 is the basic equation of radar polarimetry [18].

2.1 Ice sheet representation

For near-vertical propagation through an ice sheet, we assume that a (monochromatic) wave has its electric field components in the x and y directions of a rectangular coordinate system based in the near-horizontal surface (Fig. 1). The near-vertical plane containing the effective optic axis is taken to define the y direction [9], whose bearing is initially unknown and is one of the parameters to be determined. The rectangular coordinate system (x', y') in which the measurements are made is orientated at an angle ε to the x-axis. The ice sheet is modelled as a birefringent medium characterised by a two-way phase shift, δ, and orientation of the effective optic axis, ε. Reflection from a rough surface at near-normal incidence is described by different reflection coefficients along orthogonal axes oriented at an angle γ to the optic axis ((S,S) in Fig. 1). Although each Fresnel reflection coefficient will in general be complex, the effect on the polarisation behaviour will be given by their ratio, r (taken so that $r \geq 1$) which is assumed to be real. Backscatter of a fully polarised wave, transmitted on a linearly polarised aerial at an angle β to the x-axis and received on a linearly polarised aerial at an angle θ to the x-axis, can be described by [19]:

$$E_R(\theta) = R(\theta)\, P(\delta/2)\, R(\gamma)\, S(r)\, R(-\gamma)\, P(\delta/2) R(-\beta)\, E_T$$ (3)

where $E_R = [E_{Rx},\ 0]^T$ and $E_T = [E_{Tx},\ 0]^T$ in their respective aerial coordinate systems (Fig. 1) and

$$P(\delta) = \begin{bmatrix} 1 & 0 \\ 0 & \exp(i\delta) \end{bmatrix}, \quad S(r) = \begin{bmatrix} 1 & 0 \\ 0 & r \end{bmatrix}, \quad R(\theta) = \begin{bmatrix} \cos\theta & \sin\theta \\ -\sin\theta & \cos\theta \end{bmatrix}.$$

Here, P is the phase shift matrix, S the target scattering matrix and R the rotation matrix.
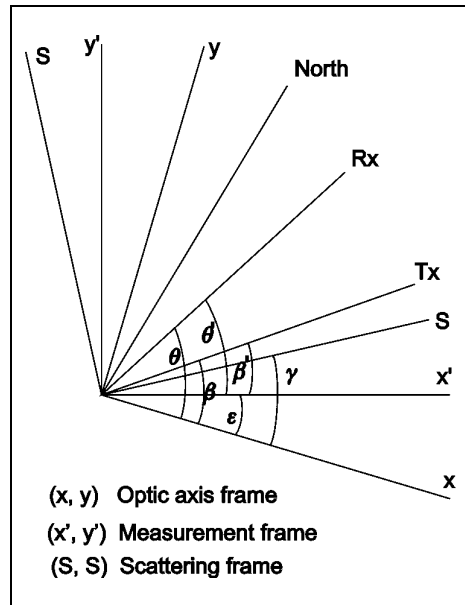

Fig. 1. *Relationship between coordinate systems for field measurements, reflecting surface and optic axis. Tx is the orientation of transmitting aerial, Rx the orientation of the receiving aerial.*

In polarimetry it is conventional to refer to orthogonally polarised wave directions as H (horizontal) and V (vertical), where for oblique incidence of a wave onto a scattering surface these directions bear some obvious relation to the directions of the transmitted E vector. Although for the near normal incidence used in glacier sounding there is no real distinction between H and V, we shall use the convention as a convenient means of distinguishing between waves transmitted along the x'-axis (H) and the y'-axis (V). For transmitting and receiving on orthogonal (e.g. linearly) polarised aerials where H is orientated at an angle ε to the x-axis, Eq.3 can be written as

$$E_R = R(\varepsilon)\,P(\delta/2)\,R(\gamma)\,S(r)\,R(-\gamma)\,P(\delta/2)\,R(-\varepsilon)\,E_T \tag{4}$$

where for brevity we write

$E_R = [H, V]^T$, $E_T = [H, V]^T$ with the understanding that only one of the H or V components is implied in any single measurement with the stated aerial system.

3 DECOMPOSITION OF SINCLAIR MATRIX

Comparison of Eqs. 1 and 4 shows that the Sinclair matrix is given by

$$S_M = \begin{bmatrix} HH & HV \\ VH & VV \end{bmatrix} = R(\varepsilon)P(\delta/2)R(\gamma)S(r)R(-\gamma)P(\delta/2)R(-\varepsilon) \tag{5}$$

It is assumed, by Lorentz' theorem of reciprocity, that HV=VH, so S_M is symmetric. There are therefore six independent parameters that can be determined from the three complex elements of S_M.

For a three parameter model, where the ice sheet is described by two parameters, an optical axis direction ε and a phase shift δ, and the reflecting surface by a single parameter, r, the ratio of reflection coefficients in the two orthogonal directions parallel and perpendicular to the optic axis, all three can be found directly from a (con)eigenmode analysis. However, we find that three parameters are insufficient to fit the measurements and another one is required. There are cross-polarisation terms which can be accounted for by allowing the principal axes of the reflecting surface to be oriented at an angle γ to the optic axis. While this modification is not the only way of introducing the cross-polarised terms (for example, it is mathematically equivalent to having non-zero off-diagonal terms in the (symmetric) target scattering matrix S) it has the advantage of having a simple physical interpretation which can be easily visualised and related to real surfaces.

An iterative/analytical method has been used to decompose the scattering matrix S_M into its constituent matrices to give the values of the 4 parameters (γ, ε, ρ, δ). An 'absolute' amplitude and phase (R, f) can also be calculated, which can be considered as a normalising factor for the scattering matrix.

We find that there is also a set of 'complementary' solutions ($\pm\pi/2 - \gamma$, $\varepsilon \pm\pi/2$, ρ, $2\pi-\delta$) whose polarisation response or signature [15] has the same amplitude pattern but differs in phase by the amount, δ. The matrix S_{MC} formed by using the complementary values in Eq. 5 above for S_M:

$$S_{MC} = R(\varepsilon + \pi/2)\,P(\pi-\delta/2)\,R(\pi/2 - \gamma)\,S(r)\,R(-\pi/2 + \gamma)\,P(\pi-\delta/2)\,R(-\varepsilon - \pi/2)$$

is related to S_M by

$$S_M = S_{MC}\exp(i\delta).$$

The need for complementary solutions is revealed when field data are analysed. When calculating parameter values over a continuous range of depths, the iterative/analytic solution method produces sudden jumps in the values of the parameters γ, ε, and δ. However, if the complementary solutions are calculated as well, the jumps are shown to be transitions between double-valued parameters (Fig. 2). The value of r is single valued, as reciprocal values of r do not affect the solution procedure. In a forward model, but not with real data, it is possible to distinguish between the 'real' and 'complementary' solutions.
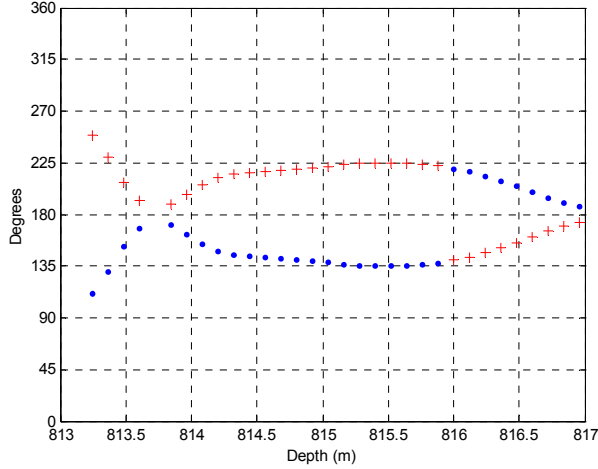
Fig. 2. *Plot of phase shift introduced in two-way path through the ice. There are two solutions to the scattering matrix, δ (dots) and 2π–δ (crosses), both of which are needed to give a continuous variation of phase with depth.*

3.1 Coneigenmode analysis

Complementary solutions may be connected with the fact that Eq. 2 always has two orthogonal solutions for **x** if the scattering matrix is symmetric [20]. We solve Eq. 2 by writing it in the form [16, p245],

$$(S_M S_M^*)\, \mathbf{x} = |\lambda|^2\, \mathbf{x}$$

where S_M^* is the component-wise conjugate of S_M, which shows that the (positive) square roots of the eigenvalues of $S_M S_M^*$ are the coneigenvalues of S_M and the eigenvectors of $S_M S_M^*$ are the coneigenvectors of S_M. The form of the equation shows that for arbitrary ϕ the matrix $S_M \exp(i\phi)$ will have the same coneigenvectors and coneigenvalues as S_M. There is also an inherent phase indeterminacy of the coneigenvalues arising from the nature of Eq. 2 [14]. If **x** is a solution and λ is a coneigenvalue of S_M then $\lambda \exp(2i\phi)$ is also a coneigenvalue since, for arbitrary ϕ,

$$S_M\,(exp(i\phi)\,\mathbf{x}) = \exp(2i\varphi)\,\lambda(\exp(i\phi)\,\mathbf{x})^*.$$

Not only are there an infinite number of coneigenvalues for a given (symmetric) matrix, there are an infinite number of (symmetric) matrices with the same coneigenvectors. This contrasts with ordinary eigenvalue equations, which have only finitely many distinct eigenvalues [16, p245]. Interpretation and significance of the phase indeterminacy is not fully understood [14].

Thus, the coneigenvectors and coneigenvalues of S_M and S_{MC}, are identical. The value of r (or $1/r$) can be found immediately from the coneigenvalues.

4 DATA COLLECTION AND ANALYSIS

A vector network analyser (HP8751A) was used as a step-frequency radar, transmitting a series of increasing tones (fixed frequencies with constant separation, Δf), each for a set length of time. Fourier techniques transform the signal to its equivalent pulse in the time domain. Usually a bandwidth of up to about 200 MHz was used, with transmit frequencies ranging from around 200 to 400 MHz. When processing the data, both the bandwidth and centre frequency can be adjusted. Thus we can either select the full bandwidth, which gives the highest depth resolution, or we can narrow the bandwidth and simulate the effect of moving a window across the full frequency range. This allows the frequency dependence of the scattering matrix parameters to be measured and also simulates the response of airborne radar systems, which have rather narrow bandwidths compared with the network analyser. Smaller bandwidths give less

depth resolution, acting as a smoothing filter on the derived polarisation parameters. The relationship between the observed phase shift δ and the birefringence $\Delta\varepsilon$ is given by [19]

$$\delta = (2\pi/\lambda)(n_e-n_o)2H = (2\pi/\lambda)\Delta n 2H = 2\pi Hnbf/c$$

which can be recast as

$$b= \delta c/(2\pi\, H\, n\, f) = \delta\lambda/(2\pi\, H\, n) \qquad\qquad (6)$$

where δ = phase shift measured in scattering matrix decomposition (i.e. two-way travel through the ice), H is thickness of layer, ε is the permittivity of ice, b the relative birefringence ($=\Delta\varepsilon/\varepsilon \approx 2\Delta n/n$), n the refractive index ($=\sqrt{\varepsilon}$), f the frequency of the radio waves, λ their wavelength and c the velocity of electro-magnetic waves in vacuo.

When decomposing the Sinclair matrix at a single frequency, we can only determine δ modulo 2π. However, we can take advantage of the frequency dependence of the birefringence and the wide bandwidth of the radar to resolve this 2π ambiguity and give a more accurate lower bound to the birefringence. For a given depth, the values of the optic axis direction γ and phase shift δ were calculated for different centre frequencies covering the range of the original data. We modelled the observed behaviour by a two-layer ice sheet, with each layer having a different optic axis orientation and birefringence. The model parameters were adjusted to give a close fit to the observations, without a formal optimisation procedure being used (Fig. 3). This procedure also removes the ambiguity of having complementary solutions.

5 RESULTS AND DISCUSSION

Only very preliminary results are given here, to illustrate some of the principles discussed above. We took representative sites from Rutford Ice Stream grounding zone, Korff Ice Rise and the north-west corner of Ronne Ice Shelf, and analysed the radar data using a two-layer model for the frequency dependence of the orientation of the optic axis and the phase difference, δ. Using Eq. 6 gives values of birefringence shown in Table 2. The greatest value of 0.15% is well below the value of 1.1% given for the birefringence of a single ice crystal [21], suggesting that the ice fabric is rather weak and not particularly anisotropic.

There is a clear distinction between the upstream sites (Rutford and Korff) where the birefringence is around the 0.1% level and the site near the ice front (NW Ronne) where it is about half that value. This can be understood if the lower layer of ice, with the strongest birefringence, is melting off into the sea and being replaced by randomly oriented snow crystals with a weaker fabric on the surface.

When the radar data are displayed in the time domain, the equivalent pulse reflected from the base or an internal layer can be readily identified. Different orientations of the aerial give a small spread of arrival times. This spread is related to the birefringence, as the ordinary and extraordinary wave will travel at slightly different speeds. The relationship $b = \Delta\varepsilon/\varepsilon \approx 2\Delta n/n$ shows that a 0.1% level of birefringence will give a 1 m difference in apparent depth in ice 2000 m thick.
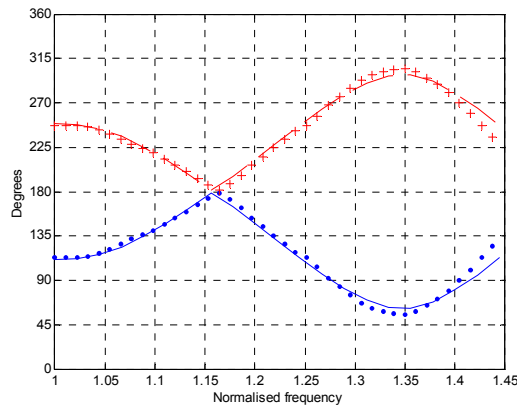

Fig. 3. *Plot of frequency dependence of phase shift introduced in two-way path through the ice. Principal values are shown by dots (measured) and continuous line (modelled); complementary values are shown by crosses (measured) and dashed line (modelled). Model parameters: top layer, phase shift 215 degrees; bottom layer, phase shift 840 degrees.*

Table 2: Polarisation parameters.

	Optic axis bearing		Phase shift		Thickness	Initial frequency	Relative birefringence
	ε_1	ε_2	δ_1	δ_2	H (m)	f_0 (MHz)	b (%)
Rutford	-40	30	50?	1400?	1570	273	.09?
Korff	-45	30	215	840	816	230	.15
NW Ronne	90	-40	50	110	399	230	.05

6 CONCLUSIONS

The vector network analyser used as a polarimeter is a very powerful instrument for investigating the structure and properties of ice sheets and their reflecting horizons, both basal and internal. The polarisation parameters are consistent with observations that echo strength can vary by 20 dB or more depending on the orientation of the transmitting and receiving aerials. This variation needs to be taken into account when attempting to interpret echo strength data gathered from systems with only a single aerial orientation. Polarisation, as well as refraction, will also have to be allowed for when it becomes feasible to gather and process SAR data of the subglacial environment. A scattering matrix approach to collecting and analysing data can be used on an airborne system, opening up the possibility of developing a polarimetric airborne SAR capable of imaging the subglacial environment, such as glacier and ice stream beds.

7 REFERENCES

1. Jiracek, G.R.1967. Radio sounding of Antarctic ice. *University of Wisconsin Geophysical and Polar Research Centre, Research Report Series No. 67*, 1-127.

2. Bogorodskiy, V.V., Trepov, G.V. and Fedorov, B.A. 1970. On measuring dielectric properties of glaciers in the field. (*In* Gudmandsen, P., ed. *Proceedings of the international meeting on radioglaciology, Lyngby, May 1970*. Lyngby, Technical University of Denmark, Laboratory of Electromagnetic Theory, 20-31.)

3. Kluga, A.M., Trepov, G.V., Fedorov, B.A. and Khokhlov, G.P. 1973. Some results of radio-echo sounding of Antarctic glaciers in the summer of 1970-71. *Trudy Sovetskoy Antarkticheskoy Ekspeditsii*, Tom 61, 151-63.

4. Clough , J.W. 1974. *Propagation of radio waves in the Antarctic Ice Sheet*. Ph.D thesis, University of Wisconsin.

5. Bentley, C.R. 1975. Advances in geophysical exploration of ice sheets and glaciers. *Journal of Glaciology*, 15(73), 113-135.

6. Woodruff, A.H.W. and Doake, C.S.M. 1979. Depolarisation of radio waves can distinguish between floating and grounded ice sheets. *Journal of Glaciology*, 23(89), 223-232.

7. Yoshida, M., Yamashita, K. and Mae, S. 1987. Bottom topography and internal layers in East Dronning Maud Land, East Antarctica, from 179 MHz radio echo-sounding. *Annals of Glaciology*, 9, 221-224.

8. Fujita, S. and Mae, S. 1993. Relation between ice sheet internal radio-echo reflections and ice fabric at Mizuho Station, Antarctica. *Annals of Glaciology*, 17, 269-75.

9. Hargreaves, N.D. 1977. The polarization of radio signals in the radio echo sounding of ice sheets. *Journal of Physics. D Applied Physics*, 10(9), 1285-1304.

10. Hargreaves, N.D.1978. The radio frequency birefringence of polar ice. *Journal of Glaciology*, 21, 301-313.

11. Musil, G.J. 1987. *Synthetic aperture radar sounding through ice*. M.Sc. thesis, University of Cambridge.

12. Musil, G.J. 1989. On the underside scarring of floating ice sheets. *Annals of Glaciology*, 12, 118-123.

13. Musil, G.J. and Doake C.S.M. 1987. Imaging subglacial topography by a synthetic aperture radar technique. *Annals of Glaciology*, 9, 170-175.

14. Lüneburg, E. 2002. Aspects of radar polarimetry. *Turkish Journal of Electrical Engineering and Computer Sciences*, 10(2), 219-243.
15. Ulaby, F.T. and Elachi, C. 1990. F.T. Ulaby and C Elachi, Eds, *Radar polarimetry for geoscience applications*. Artech House.

16. Horn, R.A. and Johnson, C.R. 1985. *Matrix analysis*. Cambridge University Press, pp561.

17. Lüneburg, E. and Cloude, S.R. 1997b. Radar versus optical polarimetry. *In* Mott, H. and Boerner, W-M, Eds, *Wideband interferometric sensing and imaging polarimetry, Proceedings of SPIE (The International Society for Optical Engineering)*, Vol 3120, 361-372.

18. Lüneburg, E. and Boerner, W.-M. 1997 Homogeneous and inhomogeneous Sinclair and Jones matrices. *In* Mott, H. and Boerner, W-M, Eds, *Wideband interferometric sensing and imaging polarimetry, Proceedings of SPIE (The International Society for Optical Engineering)*, Vol 3120, 45-54.

19. Doake, C.S.M.1981. Polarization of radio waves in ice sheets. *Geophysical Journal of the Royal astronomical Society*, 64, 539-558.

20. Lüneburg, E. and Cloude, S.R. 1997a. Bistatic scattering. *In* Mott, H. and Boerner, W-M, Eds, *Wideband interferometric sensing and imaging polarimetry, Proceedings of SPIE (The International Society for Optical Engineering)*, Vol 3120, 56-68.

21. Matsuoka, T., Fujita, S., Morishima, S. and Mae, S. 1997. Precise measurement of dielectric anisotropy in ice Ih at 39 GHz. *Journal of Applied Physics*, 81(5), 2344-48.